Journal of Advanced Engineering Trends
ISSN : 2682 - 2091

Vol. 41, No.2. July 2022

http://jaet.journals.ekb.eg

Thermal Design and Analysis of a Low Earth Orbit Micro-Satellite

Dr. Ahmed Farag, Dr. M. Elfarran[1]

1 Assistant Professor, Aeronautical Engineering Department, Institute of Aviation Engineering and Technology, Giza, Egypt

Abstract

Micro and Nano satellites are cheap, feasible and provide a platform for new technologies to be tested and validated in space which can then be extended to larger satellites for enhanced applications. Orbital harsh conditions make thermal system design very big challenge to satisfy the different operation conditions required per satellite components.

Thermal Control system (TCS) analysis of A Remote Sensing Micro-Satellite is crucial in its conceptual design phase. The thermal system design concept of the Micro-Satellite may be passive or active. Satellite thermal control system shall provide suitable temperature envelop allow components to work in full performance. It consumes daily average power about 50 W. Battery is the most critical component because of its capacity sensitivity to temperature changes.

This work deals with passive thermal system performance applied to a Sun-Synchronous Micro-Satellite with two deployed solar cells in Low Earth Orbit (LEO) at 668 km altitude. Operating thermal envelope of satellite on-board components is introduced. Thermal design of the satellite is created to demonstrate the use of computer software for thermal analysis.

Satellite thermal analysis is performed by Thermal desktop / SINDA FLUINT Software to ensure that the satellite electrical equipment temperatures maintained in the required ranges for normal operation.

Keywords

Passive thermal control, orbit, remote sensing, coating, micro-satellite, and thermal design

1. INTRODUCTION

In the following paper Thermal Analysis was done for a sun-synchronous Micro-satellite. Its size is 550 x 550 x 350 mm³. The Micro-satellite splits into two Parts: the Unified Bus Structure, and the Payload (Camera) [1]. Passive thermal control system are used. Study the effect of different types of coating and insulators are performed by changing their physical and optical properties.
Thermal Analysis is done by solving of thermal budget equation numerically to determine external fluxes and its effects on the temperature of Micro-satellite subsystems in orbit. Thermal Desktop/Fluint software was used for geometry drawing, thermal analysis and simulation for worst cases during its lifetime.
Heat Fluxes, and Temperatures are calculated for the solar cells, for each side of the Micro-satellite, and for internal components using.

Katelyn Boushon Spring 2018 [2], presented the case study involves the construction of multiple revisions of the potential satellite thermal model. The analysis results demonstrated how increasing model complexity and nodal resolution affect resulting satellite temperatures. The passive thermal control method of manipulating satellite surface optical properties is used to raise the satellite component temperatures to the necessary range.

A. M. Elhady 2010 [3], studied the effect of thermal contact resistance in design calculations on satellite thermal envelope and evaluated the satellite thermal control subsystem efficiency. Results of a theoretical study showed that the satellite thermal envelop has no respect changes from the qualitative point of view; quantitatively small changes of no more than 1°C are detected in few places of structure joint interfaces.

Received:12 Decamber, 2020, Accepted:3March, 2021

Millan Diaz-Aguado et al. 2006 [4], performed Thermal cycling and thermal analysis for small satellites. The thermal cycling was done in Chamber-N at Johnson Space Center, Texas, using worst case hot and cold scenarios. The thermal analysis was conducted using Finite Elements (FE), and the results were compared to the test data and validated. FASTRAC is planned to be in a LEO orbit which ranges between 300km and 500km in altitude. The orbits were then simulated to determine the characteristics of the LEO orbits in which FASTRAC can survive.

S. Corpino et al. 2015 [5], presented the process and the results of the thermal analysis applied to a nanosatellite developed at Politecnico di Torino. First, main mission parameters and the spacecraft design are presented, in order to fix the boundary conditions and the thermal environment used for the analysis. Then, the thermal model built to solve the thermal balance problem is described into details, and the numerical simulation code is presented. Finally, results are given and discussed in depth. The tool developed provides excellent modelling capabilities and temperature distributions have been validated through commercial software.

Nomenclature

Symbol	Quantity
F_i	Area (node i) [m^2]
e_i	Emissivity factor [-]
K_{ij}	Heat transfer by conduction [W/K]
σ_0	Stefan-Boltzmann constant [=$5.67.10^{-8}$ $W/m^2/K^4$]
q_S	Incident Solar flux and albedo [W/m^2]
q_{SB}	Solar Cells flux [W/m^2]
C_i	Thermal capacitance (node i) [J/K]
Q_{diss}	Heat rejection from equipment [W]
Q_I	Heat rejection (node i) [W/m^2]
Q_a	Solar albedo [W/m^2]
q_E	Earth infra-red (IR) [W/m^2]
εHij	Heat transfer by radiation [m^2]
Q_s	Incident sun flux [W/m^2]

Q_T	Earth infra-red [W/m^2]	
A_{si}	Absorptivity factor (node i)	[-]

Abbreviations

TCS	Thermal Control Subsystem
LEO	Low Earth Orbit
IR	Infrared
PCU	Power Control Unit
CDH	Command and Data Handling
TTC	Telemetry Tracking and Command

1. GOVERNING EQUATIONS & THEORY:

- Thermal control inside the satellite is interacted by heat transfer concept as conduction, radiation, and no convection:
- Conduction between thermal node and its adjacent nodes
- Radiation among thermal nodes (include space)
- Q_{in}: Heat Dissipation
- Q_{orbit}: Orbital Fluxes

- The thermal balance equation in transient case was solved by software tool called Thermal Desktop/Sida Fluint [6,7, 8].The energy balance terms in the equation are stated as:

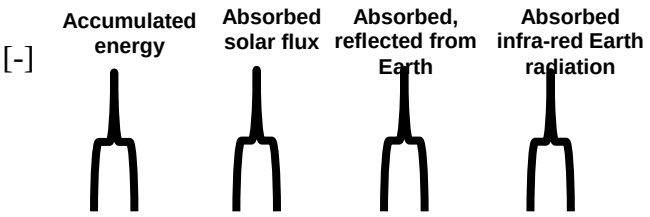

$$C_i \cdot \frac{dT_i}{dt} = A_{si} \cdot F_i \cdot Q_s + A_{si} \cdot F_i \cdot Q_a + \varepsilon_i \cdot F_i \cdot Q_T +$$

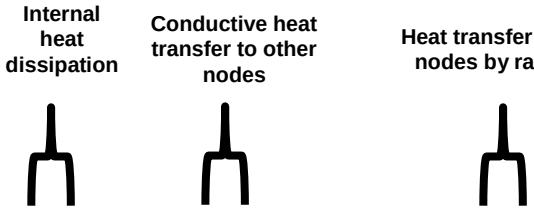

$$Q_i + \sum_j K_{ij} \cdot F_i \cdot (T_j - T_i) + \sum_j \sigma_0 \varepsilon \cdot H_{ij} \cdot (T_j^4 - T_i^4) \quad (1)$$

1.1 HEATERS POWER CALCULATIONS (Q_{HEATER}) :[9]

Power consumption of heaters is calculated at the minimum values of external fluxes, and the minimum number of operating devices (minimum heat dissipation) as shown in (Equ. 2), by using the calculated radiator area from (Equ. 3) to be able to compensate the heat losses inside satellite during Eclipse.

$$Q_{in\text{-}min} + Q_{Heater} = \varepsilon \sigma T^4 F_{rad} \quad (2)$$

1.2 RADIATOR AREA CALCULATIONS (F_{RAD}) : [10,11]

Radiator area calculations of the satellite panel which many devices fixed on and have heat dissipation are necessary to keep the heat

balance between inside and outside the satellite. By applying Thermal Budget Equation (Equ. 1) at maximum external solar fluxes, maximum heat dissipation, and after simplification as shown in (Equ.s 3,4), we can calculate the radiatior area which is suitable for our design.

$$q_S A_s F_{rad} + q_E \varepsilon F_{rad} + Q_{in} + q_{SB} \varepsilon F_{rad} = \varepsilon \sigma T^4 F_{rad} \quad (3)$$

$$q_S = q_{Solar} + q_{Albedo} \quad (4)$$

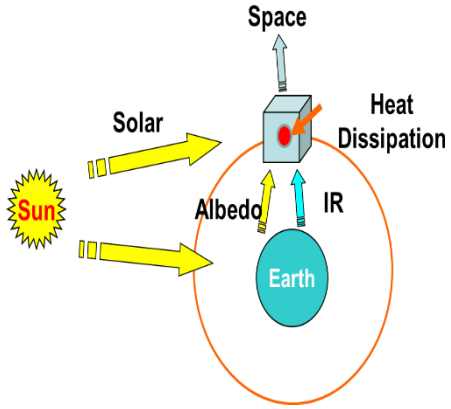

Figure 1: Satellite External & Internal Heat Balance

2. NUMERICAL AND THERMAL ANALYSIS

2.1 Thermal Model:

Thermal modeling of a sun-synchronous Micro-satellite with two deployed solar cells its size is 550x350 mm for each in LEO, at 668 km altitude is performed by Thermal desktop/Fluint Software as shown in figure (2), to study the effect of different types of coating and insulators by changing their physical and optical properties [12, 13]. The dimensions of the six panels of the Micro-satellite are shown on table 1.

Table 1 : Satellite Dimensions

Orientation	Dimensions Structure Panels (mm)
Z+ Payload	550x350
Z-	550x350
Y+ Adaptor	550x550
Y-	550x550
X+ Flight Direction	550x350
X-	550x350

The payload bay sitting on top of the bus structure and not being integrated in the satellite, its design concept using the approach with a large telescope that is capable of 60 cm GSD from 668 km orbit.

-Payload Volume of 550x350x650mm.
-Payload Mass of 40kg.
-Payload Average Power 50W.

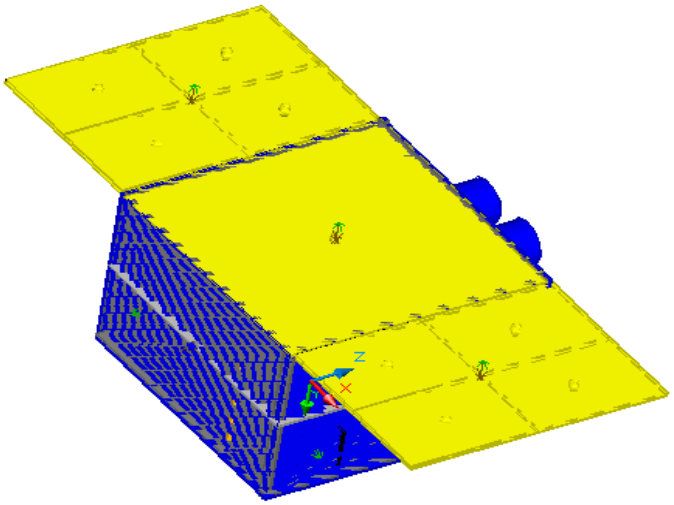

Figure 2:Satellite External Configuration

Thermal analysis is performed for the Micro-satellite to study the worst cases that exposed to [14, 15, 16] during both satellite positions (Sun Pointing and Shooting). Hot Case which is the

external heat fluxes (Solar , Infrared (IR), Earth albedo, and Solar cells view factors) is maximum, and in cold case (Eclipse) is minimum as shown in Figures (3, 4). The temperature inside the Micro-satellite should be maintained in the specified range for each subsystem.

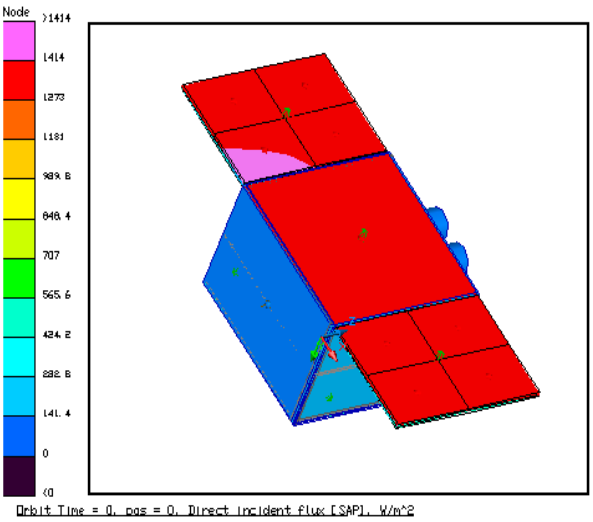

Figure 3: Miro-Satellite External Heat Fluxes in Sun Pointing Position

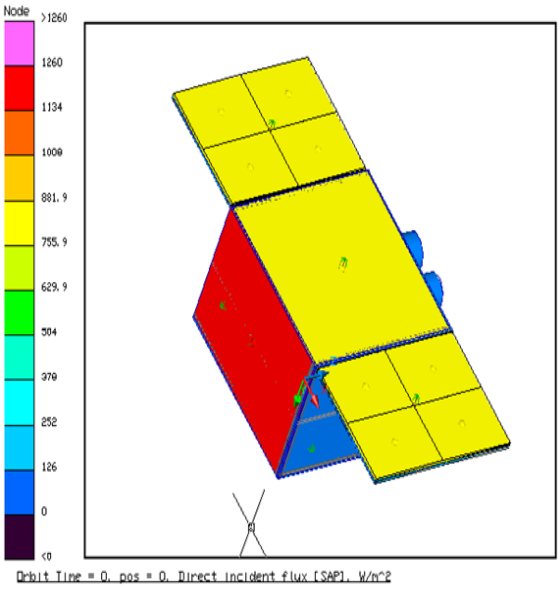

Figure 4: Miro-Satellite External Heat Fluxes in Shooting Position

2.2 Material Properties

Aluminum is the material used for satellite body; Carbon Fibers are used for Solar panels. Physical and Optical Properties as shown in tables (2,3) [17, 18, 19]:

Table 2 : Thermophysical properties

Type	Thermal Conductivity ((W/m.k)	Density (Kg/m3)	Specific Heat ((J/Kg.K)
Carbon Fibers	1200	1700	2000
Aluminum	237	2700	800

Table 3 :Optical properties

Type	Absorptivity (α)	Emissivity (ε)
Black Anodized	0.9	0.88
Solar Cells	0.9	0.89

2.3 External Heat Loads

Heat Loads are commonly from[20, 21]:

- The Sun: Input solar flux 1414 $\frac{W}{m^2}$
- Albedo: 29% of direct solar flux energy.
- The Earth Infrared: 257 K.
- Conductivity between Solar Cells and panel are 30 W/m^2k.
- Space environment temperature is 4K.

2.4 Internal Heat Dissipation

Internal heat dissipation for the satellite subsystems are shown in table 4:

Table 4 : Internal heat dissibation

Pakage/Subsystem	Heat Dissibation
Power Supply	55W
Payload	40W

Attitude Orbit Control	50W
Telemetry Command and Tracking	30W
On Board Data Handling	15W

2.5 Temperature Requirements

Temperature ranges for the satellite components are shown in table 5:

Table 5 : Temperature ranges

Item	Temperature Requirment
Electric Equipment	-15 : +45 °C
Battery	-15 : +35 °C
Payload (Camera)	-10 : +45 °C
Antenna	-100 : +80 °C
Solar Arrays	-90 : +90 °C

2.6 Orbital parameters

Orbit Parameters for both Hot and Cold cases are shown in table 6:

Table 6 :Orbit Parameters

Parameter	Cold Case	Hot case
Altitude (Km)	668	668
Beta Angle (β)	22^0	27^0
Solar Flux (W/m^2)	1322	1414
No# of revolutions	6	12

2.7 BOUNDARY CONDITIONS

The software solves the thermal balance equation in transient case in both sun pointing, and shooting mode with orbital parameters and material properties as shown in tables (2,3,6). The initial temperature of radiation surface is 20 °C.

2.8 MODEL ANALYSIS

- The software Thermal Desktop is used to accomplish satellite analysis.
- Thermal model algorithm is used the finite difference method.
- Analysis model nodal number is about 2000~3000.

2.8.1 Hot case Scenario

Hot case was considered at Beta angle (**β** = 27^0) as shown in figure (4,5), which all devices are turned on and maximum external heat fluxes, and the radiation surface has minimum absorbtivity and maximum emissivity factors.

Hot case was analyzed for -Y axis is pointing to the sun for the first 6^{th} revolutions, then +Z axis will be pointing to Nadir, for starting imaging mode for 10 minutes at the beginning of the 7^{th} and 8^{th} revolutions, then back again to the direction which -Y axis is pointing to the sun. Hot Case scenario is shown in table (7). Temperatures was calculated on the satellite side panels, solar cells, and for internal components.

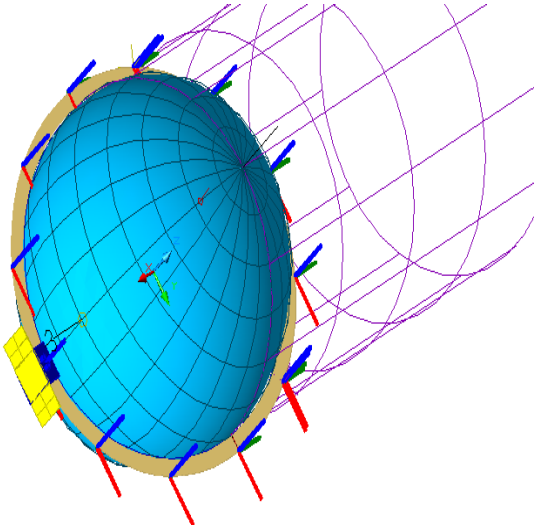

Figure 5: Sun Pointing Mode at β= 27°

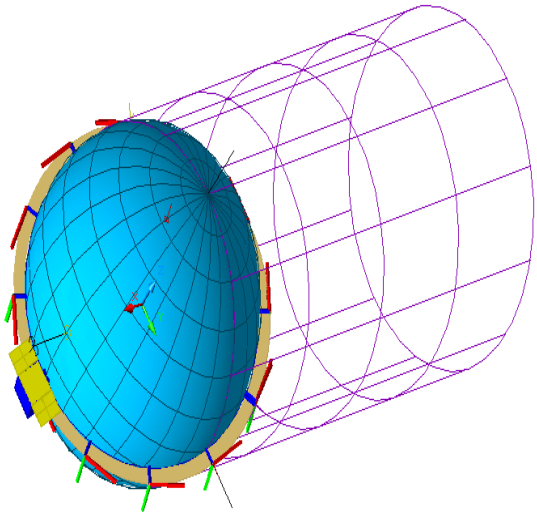

Figure 6: Shooting Mode at β= 27°

Table 7: Hot Case Scenario

Time	Orbit
0 s - 41203.6 s	Sun Pointing
41205 s - 41803.6 s	Shooting
41804 s - 47089.8 s	Sun Pointing
47090 s – 47690.8 s	Shooting
47691 s - 70634.8 s	Sun Pointing

2.8.2 Cold Case Scenario

Cold case was considered at Beta angle (β = 22^0) as shown in figure (6), which almost all devices are turned off.
Cold case was analyzed that -Y axis is pointing to the sun for the first 6th revolutions. All devices are turned off except PCU, CDH, TTC, and X-Band transmitter are turned on during the simulation. Cold case scenario is shown in table (8). Temperatures was calculated for internal components for the main subsystems in the satellite to confirm that it is in its specified ranges.

Table 8: Cold Case Scenario

Time	Orbit
0 s - 41203.6 s	Sun Pointing

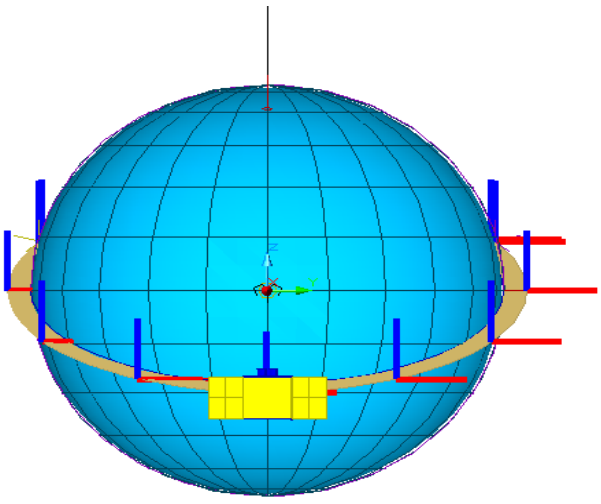

Figure 7:Sun Pointing Mode at β= 22°

3. RESULTS

3.1 Hot Case Scenario Results

The achieved results are shown in figures (8 to 15).

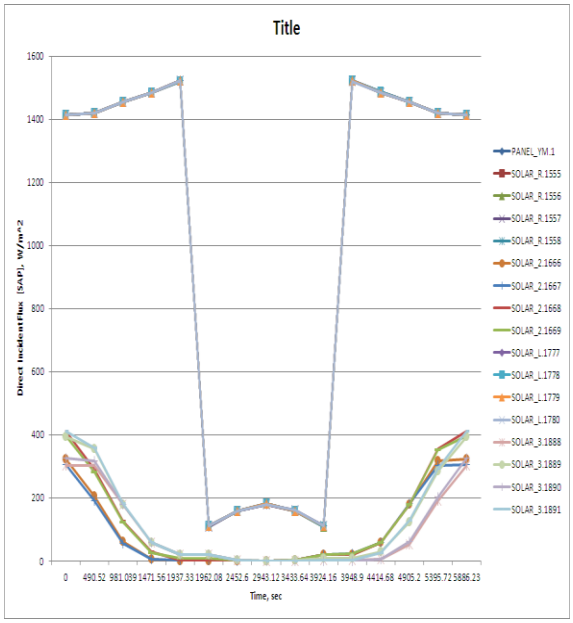

Figure 8: Heat Flux Distribution on the Solar Cells surfaces

(Sun Pointing Mode)

Figure 8 shows the heat flux values w.r.to time for all nodes of the solar cells surfaces during the mission. The maximum heat flux reflects the value of solar fluxes when solar cells is directly to the sun in the sun pointing mode. and then decreased during shooting mode at the beginning of the 7^{th}, and 8^{th} revolutions for 10 minutes.

.

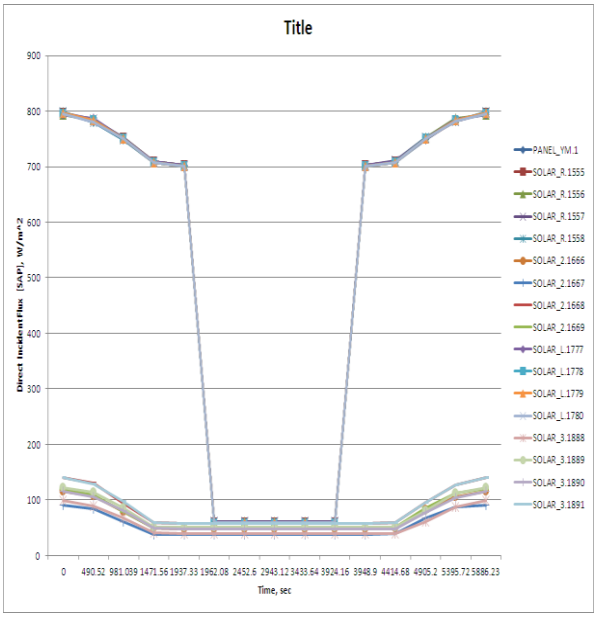

Figure 9: Heat Flux Distribution on the Solar Cells surfaces

(Shooting Mode)

Figure 9 shows the heat flux values w.r.to time for all nodes of the solar cells surfaces during the mission. The maximum heat flux reflects the value of solar fluxes when solar cells is not directly to the sun in the shooting mode. This value is lower than the one in figure (8), whih is logic because in this mode the payload camera is directly to nadir for imaging, and solar cells is not facing directly to the sun.

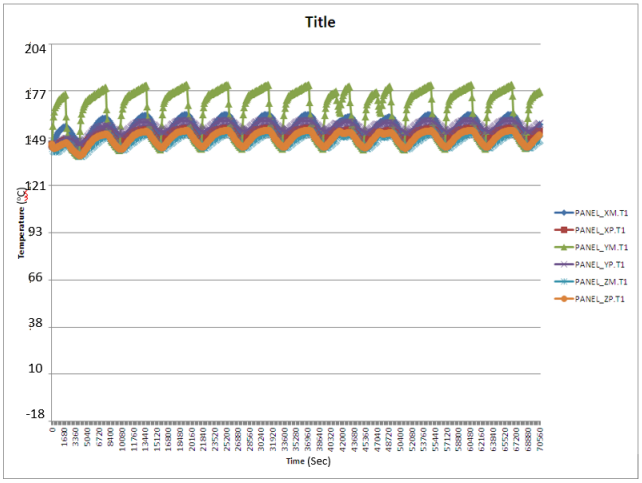

Figure 10:Temperature Values Distribution on the interior surface of Structure Panels (°C)

Figure 10 shows the temperatures ranges for internal devices vary from 0 to 52 °C which is normal, and the one in green color is higher because it is lower surface of the middle solar cells panel which is directly faces to the sun.

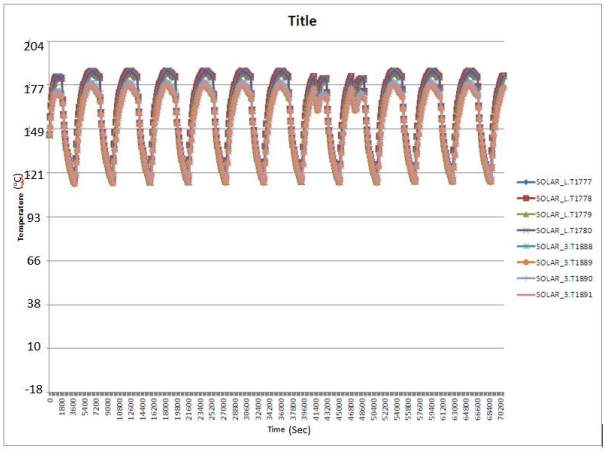

Figure 11: Temperature Values Distribution on the Left Solar Cells surfaces (°C)

Figure 11 shows the temperatures ranges for the left solar cells surfaces which is high because it is located directly to the sun.

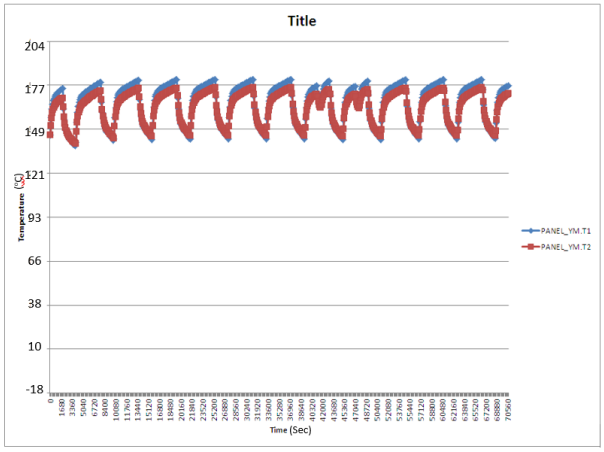

Figure 12: Temperature Values Distribution on the Middle Solar Cells surfaces (°C)

Figure 12 shows the temperatures ranges for the middle solar cells panel which is high because it is located directly to the sun.

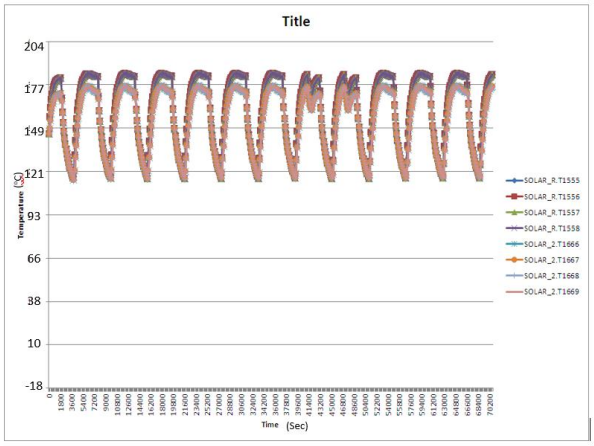

Figure 13: Temperature Values Distribution on the Right Solar Cells surfaces (°C)

Figure 13 shows the temperatures ranges for the right solar cells panel which is high because it is located directly to the sun.

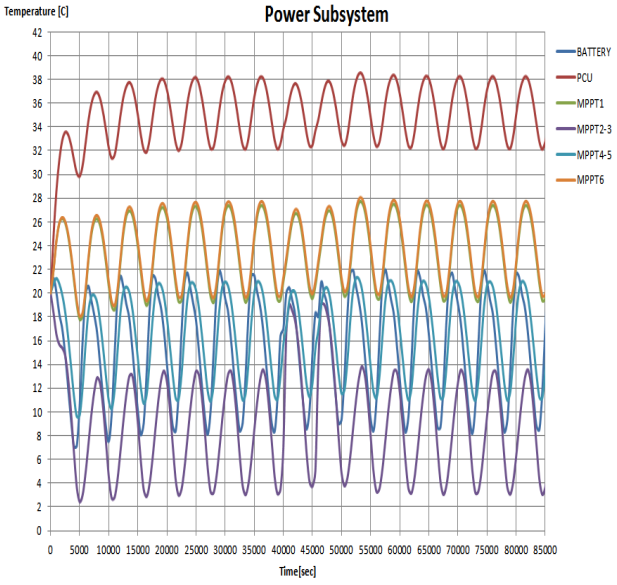

Figure 14: Temperature Values Distribution on Power subsystem devices

Figure 14 shows the temperatures ranges for internal devices for power supply subsystem which is vary from 2 to 37 °C which is good for normal and safe operation for battery.

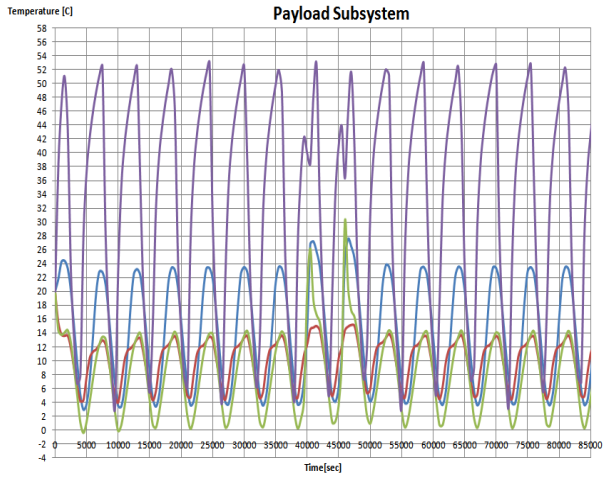

Figure 15: Temperature Values Distribution on Payload subsystem devices(°C)

Figure 15 shows the temperatures ranges for internal devices for payload (camera) subsystem which is vary from 0 to 52 °C which is good for normal and safe operation for good imaging processes.

3.2 Cold Case Scenario Results

The achieved results are shown in figures (15 to 17).

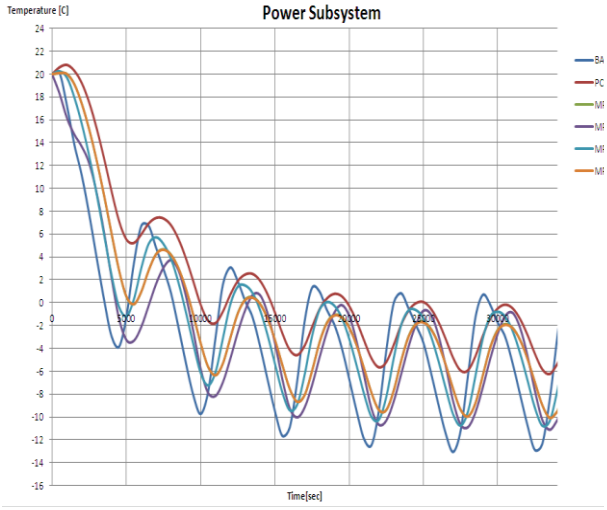

Figure 16: Temperature Values Distribution on Power subsystem devices(°C)

Figure 16 shows the temperatures ranges for internal devices for power supply subsystem which is vary from -10 to 22 °C which is good for normal and safe operation for battery.

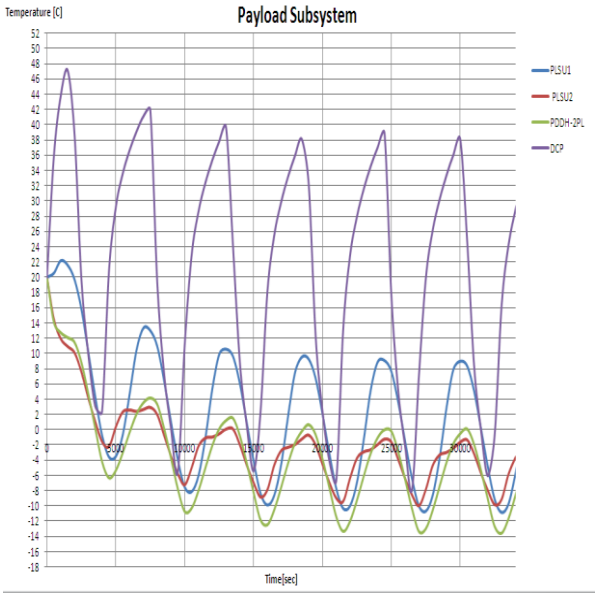

Figure 17: Temperature Values Distribution on Payload subsystem devices(°C)

Figure 17 shows the temperatures ranges for internal devices for payload (camera) subsystem which is vary from -13 to 52 °C which is good for normal and safe operation for good imaging processes.

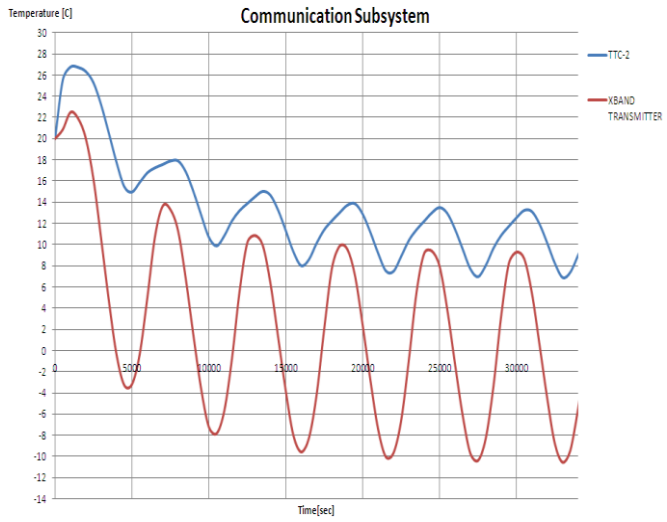

Figure 18: Temperature Values Distribution on Communication subsystem devices(°C)

Figure 18 shows the temperatures ranges for internal devices for communication subsystem which is vary from -10 to 27 °C which is good for normal and safe operation.

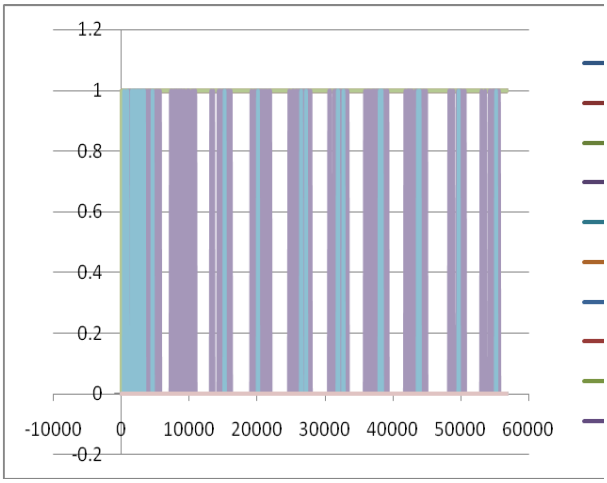

Figure 19: Heaters ON/OFF cycling (Cold Case)

Figure 19 shows the number of on/off heaters cycling during the mission when the satellite will be in cold case (Eclipse) , because it reflects the temperature stability on the internal surface of the panel.

4. CONCLUSIONS

1. Thermal Desktop/Sinda Fluint Software is a perfect tool to create satellite thermal geometry, design, analysis, and calculate temperature values, radiators area, and power of heaters for the structure panels.

2. The results were shown that thermal control system design and analysis are important to maintain all the subsystems devices in the specified ranges during all the lifetime.

3. Materials selection and using different thermal and physical properties was important to reach the optimum design for thermal control system.

4. The thermal model ensures the design requirements, and guaranteed the performance of the satellite thermally during its lifetime.

5. Finally, The maximum and minimum temperature is in range for all the devices and subsystems inside the micro-satellite.

5. REFERENCES

1. Gilmore, David G., "Spacecraft Thermal Control Handbook" Fundamental Technologies,2nd Ed, Volume I, The Aerospace Press, El Segundo, CA., 2002.
2. Elizabeth Boushon Spring "Thermal analysis and control of small satellites in low Earth orbit" 2018.
3. A. M. Elhady "Design and analysis of a LEO micro-satellite thermal control including thermal contact conductance" 2010.
4. Millan Diaz-Aguado et al., "Small satellite thermal design, test, and analysis", 2006.
5. S. Corpino et al., "Thermal design and analysis of a nanosatellite in low earth orbit", 2015.
6. O M Alifanov, A V Nenarokomov et al., Study of multilayer thermal

insulation by inverse problems method ActaAstronautica 65 pp 1284-1291, 2009.

7. Bapat S L, Narayankhedkar K G et al., Experimental investigations of multilayer Insulation Cryogenics, Vol 30, 1990.
8. Bapat S L, Narayankhedkar K G et al., Performance prediction of multilayer insulation Cryogenics Vol 30, 1990.
9. Taig Y, Bum S, Jang J et al., Numerical study of the spacecraft thermal control hardware combining solid liquid phase change material and a heat pipe Aerospace Sci and Tech 27 pp 10 16, 2013.
10. Wesley J, Thermal analysis of low layer density multilayer insulation test results AIP Conference Proceedings pp 1434- 1519, 2012.
11. L E Mavromatidis, A Bykalyuk, Mohamed E M, P Michel et al., Numerical insulation, Building and Environment 49 pp 227-237, 2012.
12. J. H. Ferziger John Wiley et al., "Numerical Methods for Engineering Applications" New York, 1981.
13. J. P. Holman, "Heat Transfer, 4th ed." (McGraw-Hill Inc., New York), 1976.
14. F. Kreith, "Principles of Heat Transfer, 3rd ed." (Intext Educational Publishers, New York), 1976.
15. Williams, Andrew., "Robust Satellite Thermal Control Using Forced Air Convection Thermal Switches for Operationally Responsive Space Missions" Master's Thesis, University of Colorado, Department of Aerospace Engineering Sciences, Boulder, CO., 2005.
16. G. D. Smith, "Numerical Solution of Partial Differential Equations" (Oxford University Press, Oxford, United Kingdom), 1978.
17. D. S. Burnett, "Finite Element Analysis" (Addison-Wesley Publishing Co.), 1987.
18. R. Siegel and J. R. Howell, "Thermal Radiation Heat Transfer" (Hemisphere Publishing Corp. New York), 1981.
19. L. Lapidus and G. F. Pinder, "Numerical Solution of Partial Differential Equations in Science and Engineering" (John Wiley and Sons, New York), 1982.
20. Robert D. Karam, "Satellite Thermal Control for System Engineering", 1998.
21. B. A. Cullimore, "Computer code SINDA '85/FLUINT System Improved Numerical Differencing Analyzer and Fluid Integrator", Version 2.3 (Martin Marietta), 2010.